Synthesis and Optical Properties of Poly{(4-nitrophenyl)-[3-[*N*-[2-(methacryloyloxy)ethyl]-carbazolyl]]diazene}

M. S. Ho,[†] C. Barrett,[‡] J. Paterson,[†] M. Esteghamatian,[‡] A. Natansohn,*[,†] and P. Rochon[‡]

Department of Chemistry, Queen's University, Kingston, Ontario, Canada, K7L 3N6, and Department of Physics, Royal Military College, Kingston, Ontario, Canada K7K 5L0

Received September 21, 1995; Revised Manuscript Received April 1, 1996[⊗]

ABSTRACT: Poly{(4-nitrophenyl)-3-[*N*-[2-(methacryloyloxy)ethyl]carbazolyl]]diazene} was prepared and its photoinduced birefringence, diffraction grating, and photorefractive asymmetric two-beam gain coupling were studied. The monomer was obtained by performing azo coupling in a two-phase water−dichloromethane system in the presence of a phase transfer catalyst. Photoinduced birefringence of up to 0.09 was observed and diffraction efficiencies of up to 25% were obtained, with atomic force microscopy studies revealing that the grating profile exhibited a sinusoidal shape. Asymmetric two-beam coupling is observed, indicating photorefractive properties, but the energy transfer phenomena are more complex, involving also diffraction by the photoinduced gratings. The combination of these three optical properties—photoinduced birefringence, surface gratings, and two-beam coupling—is believed to be unique and may eventually produce an all-optical device built of a single polymer film.

Introduction

Azo-aromatic polymers have received much attention in the past few years because of their potential uses in various optical applications, i.e., nonlinear optics, optical information storage, and optical switching.[1] Amorphous polymers containing side chain azobenzene groups have been demonstrated to be attractive candidates for reversible optical storage,[2−6] and, more recently, we found that diffraction gratings with efficiencies of up to 45% can be created in the azo polymer thin film by interference of circularly polarized laser beams.[7] Similar results were reported by Tripathy's group.[8] In addition, the photoinduced poling of nonlinear optical polymers containing azo chromophores has also been demonstrated.[9−11] Since the discovery of the photorefractive effect in organic polymers,[12] carbazole-based polymers[13−17] have attracted much attention because of their photoconductivity. Most recently, a poly(*N*-vinylcarbazole)-based polymer composite with high azo chromophore concentration (50 wt %) was prepared. A net two-beam coupling (2BC) gain of more than 200 cm^{-1} and a diffraction efficiency near 100% were reported.[18] This 2BC gain, as with most reports of photorefractivity, was achieved with a composite material doping small-molecule electrooptic chromophores, charge transporters, and charge trappers into a poly(*N*-vinyl carbazole) matrix. These optical properties illustrate the wealth of possibilities offered by azo polymers.

We are studying the reversible optical storage properties and formation of diffraction gratings for polymers with different side chain azobenzene structures. In an attempt to optimize optical and holographic storage capabilities, we have been investigating the effect of the size and dipole moment of the azo groups on the optical properties. We found that the writing and relaxation curves can be described by biexponential functions,[19] and that the writing and relaxation behavior can be characterized by rate constants of the fast and slow modes. Our polymers already contain most of the necessary elements for photorefractivity (electrooptic chromophore, charge traps, and ability to be photopoled); thus polymers with azocarbazole moieties in the side chain providing the charge transport properties necessary for photorefractivity would be of special interest.

A carbazole ring, replacing the aliphatic amine used previously,[2] should also improve the thermal and orientational stability of the azo moiety, as was demonstrated on all-aromatic amines which are part of the azo groups on the side chain of polymers.[20, 21]

Another potential benefit of having a carbazole moiety in the polymer is the possibility of building variable spacers between the main chain and the azo group, thus allowing increasing degrees of order as the azo group becomes more and more decoupled from the main-chain motion. Spontaneous ordering plays a very important role in photoinduced birefringence,[6] and by increasing the spacer, it can be systematically studied.

To our best knowledge, polymers with pendant azocarbazole moieties have not been reported previously. This may be due to the fact that carbazole is not sufficiently reactive to couple with diazotized amines under aqueous media.[22] However, it has been reported that the coupling was more efficient in a two-phase water−dichloromethane system containing a phase transfer catalyst.[22, 23] By performing the coupling under similar conditions, we obtained a fairly high yield of the coupling product. Using this synthetic approach, the spacer length between the backbone and the azocarbazole group can be easily varied, therefore allowing the possibility to control the properties of the polymer. In this report, the synthesis, optical storage properties and the formation of diffraction gratings of the novel poly{(4-nitrophenyl)-[3-[*N*-[2-(methacryloyloxy)ethyl]-carbazolyl]]diazene} (pCARBA) are presented. We also report asymmetric 2BC as proof of the photorefractive effect in this homopolymer, where all of the necessary elements for photorefractivity have been incorporated into a single monomer. Our samples also exhibit multiwave mixing beam amplification, due to the pres-

[†] Queen's University.
[‡] Royal Military College.
[⊗] Abstract published in *Advance ACS Abstracts,* May 15, 1996.

S0024-9297(95)01432-X CCC: $12.00 © 1996 American Chemical Society

Scheme 1

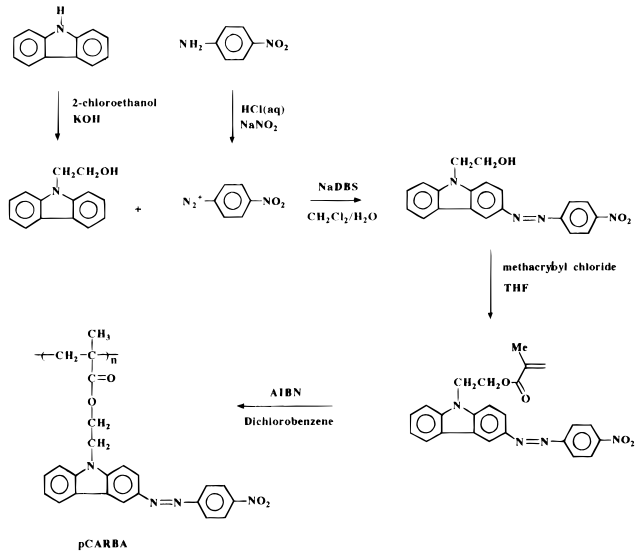

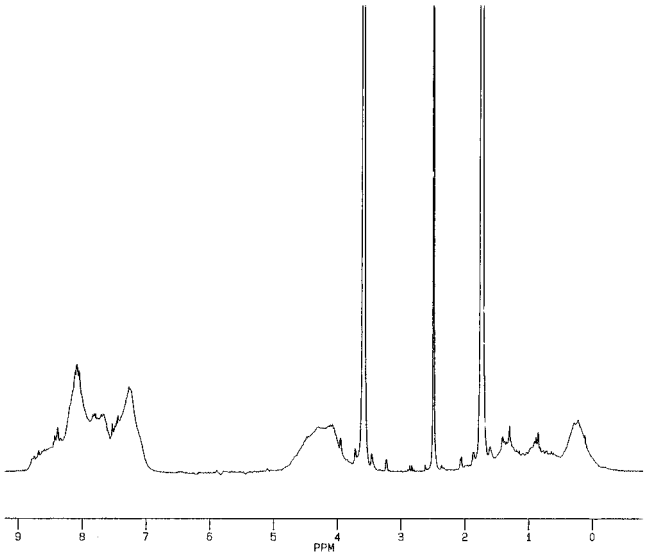

Figure 1. ^{1}H-NMR spectrum of pCARBA in THF-d_8.

ence of photoinduced gratings. The two phenomena allow the use of the polymer film as an optical switch.

Experimental Section

The proton spectra were recorded on a Bruker AC-F 200 NMR spectrometer. The ^{13}C-CPMAS-NMR spectrum of pCARBA was obtained on a Bruker ASX-200 spectrometer operating at 50 MHz with a 3.7 μs proton pulse and 2 ms cross-polarization time. The spinning rate was 3 kHz, and a TOSS pulse sequence was employed to suppress spinning sidebands. UV absorption spectra were obtained from a Hewlett-Packard 8452A diode array spectrophotometer. The molecular weight (relative to polystyrene) was obtained from a Waters Associates liquid chromatograph equipped with μ-Styragel columns and an R401 differential refractometer. The glass transition temperature (T_g) was obtained with a Mettler TA 3000 thermal analysis system equipped with a TC10A TA processor and DSC30 head. Film thickness was determined by interferometry. The detailed procedures for the measurement of the optical induced birefringence[2-6] and diffraction gratings[7] have been described previously.

Monomer. The monomer was prepared according to the reaction scheme shown in Scheme 1. *N*-(2-Hydroxyethyl)-carbazole was obtained by alkylation of carbazole with powdered potassium hydroxide. Coupling 4-nitrobenzenediazonium chloride with *N*-(2-hydroxyethyl)carbazole in two phase $H_2O-CH_2Cl_2$ mixture in the presence of sodium dodecyl benzenesulfonate (NaDBS) gave the desired (4-nitrophenyl)-[3-[*N*-(2-hydroxyethyl)carbazolyl]]diazene. Esterification of the azocarbazole with methacryloyl chloride gave the monomer.

***N*-(2-Hydroxyethyl)carbazole.** Powdered potassium hydroxide (14.0 g) was stirred with DMF (80 mL) at room temperature for 10 min. The mixture was then stirred with carbazole (6.6 g, 0.040 mol) at room temperature for 45 min. 2-Chloroethanol (4.0 g, 0.05 mol) was added slowly, and the resultant mixture was allowed to stir at room temperature for 10 h. The mixture was poured into water (1.2 L), and the white solid was filtered, washed with water, and air-dried. The white solid was dissolved in 70% ethanol, and the insoluble residue was filtered out. Water was added to the filtrate until the precipitation was completed. The cotton-like solid was filtered and dried under vacuum to yield 6.7 g of white solid (80%). ^{1}H NMR (acetone-d_6): δ = 4.08 (m, 3H), 4.54 (t, 2H), 7.20 (dt, 2H), 7.43 (dt, 2H), 7.62 (dd, 2H), 8.14 (dd, 2H).

(4-Nitrophenyl)-[3-[*N*-(2-Hydroxyethyl)carbazolyl]]-diazene. 4-Nitroaniline (2.8 g, 0.020 mol) was dissolved in a solution of concentrated HCl (10 mL) in water (300 mL). The mixture was cooled in an ice bath until the temperature was below 4 °C. Then a solution containing sodium nitrite (1.6 g, 0.022 mol) in water (10 mL) was added slowly to the 4-nitroaniline solution. The mixture was allowed to stir in the ice bath for 30 min. While the mixture was still kept in the ice bath, sodium dodecyl benzenesulfonate (1.0 g) was added. A solution of *N*-(2-hydroxyethyl)carbazole (8.4 g, 0.040 mol) in dichloromethane (300 mL) was added to the above mixture. The resultant mixture was stirred vigorously at room temperature for 24 h. Ethanol (200 mL) was added and the mixture was heated to remove the dichloromethane layer. The red precipitate was filtered, washed with water, and air-dried. The solid was recrystallized from ethanol/chloroform mixture (1:1 by volume) to yield 5.0 g of (4-nitrophenyl)-[3-[*N*-(2-hydroxyethyl)carbazolyl]]diazene (70%). ^{1}H NMR (acetone-d_6): δ = 4.10 (m, 3H), 4.64 (t, 2H), 7.35 (dt, 1H), 7.57 (dt, 1H), 7.76 (dd, 1H), 7.85 (d, 1H), 8.14 (m, 3H), 8.30 (dd, 1H), 8.46 (d, 2H), 8.84 (d, 1H).

(4-Nitrophenyl)-[3-[*N*-[2-(methacryloyloxy)ethyl]carbazolyl]]diazene. A solution of (4-nitrophenyl)-[3-[*N*-(2-hydroxyethyl)carbazolyl]]diazene (1.8 g, 5.0 mmol) and triethylamine (0.6 g, 6.0 mmol) was dissolved in THF (100 mL). A solution of methacryloyl chloride (0.7 mL, 5.0 mmol) in THF (5 mL) was added slowly to the above mixture. After the addition of methacryloyl chloride, the resultant mixture was stirred at room temperature overnight. The solvent was removed by rotoevaporation, and the residue was washed with a solution of sodium carbonate (1.0 g) in water (100 mL). The solid was filtered, washed with water, and air-dried. The solid was recrystallized from ethanol/chloroform mixture (2:1 by volume) to yield 1.5 g (70%) of (4-nitrophenyl)-[3-[*N*-[2-(methacryloyloxy)ethy) carbazolyl]]diazene. ^{1}H NMR (acetone-d_6): δ = 1.72 (t, 3H), 4.64 (t, 2H), 4.91 (t, 2H), 5.49 (m, 1H), 5.85 (m, 1H), 7.35 (dt, 1H), 7.57 (dt, 1H), 7.76 (dd, 1H), 7.85 (d, 1H), 8.14 (m, 3H), 8.32 (dd, 1H), 8.46 (d, 2H), 8.84 (d, 1H). Anal. Calcd for $C_{24}H_{20}N_4O_4$: C, 67.28; H, 4.71; N, 13.08. Found: C, 66.56; H, 4.68; N, 12.93.

Polymer and Polymer Films. The polymerization was carried out in 1,2-dichlorobenzene with 10% by weight 2,2′-azobis(isobutyronitrile) (AIBN) as initiator. The monomer was allowed to polymerize under argon at 60 °C for 2 days. The polymerization was stopped by pouring the reaction mixture into ethanol. The polymer was redissolved in THF, precipitated again in ethanol, and finally dried under vacuum. Anal. Calcd for $C_{24}H_{20}N_4O_4$: C, 67.28; H, 4.71; N, 13.08. Found: C, 65.85; H, 4.59; N, 12.47. A ^{1}H-NMR spectrum of pCARBA in THF-d_8 is shown in Figure 1 and presents the typical resonances of the aromatic protons (7−9 ppm), the NCH_2CH_2O group (3.8−4.7 ppm), the main-chain methylene group (1−2 ppm), and the α-methyl protons (0.2 ppm). Since the solubility of pCARBA in most solvents is fairly limited, a ^{13}C-NMR spectrum of it was obtained in the solid state. The ^{13}C-CPMAS-NMR spectrum is shown in Figure 2 and its assignments are as follows: 180 ppm-carbonyl; between 170 and 150 ppm, resonances of carbons bound to nitrogen in the azocarbazole group; 145 ppm, carbons 1a and 8a of the carbazole; 125 ppm, all protonated carbons of the azocarbazole (except 1

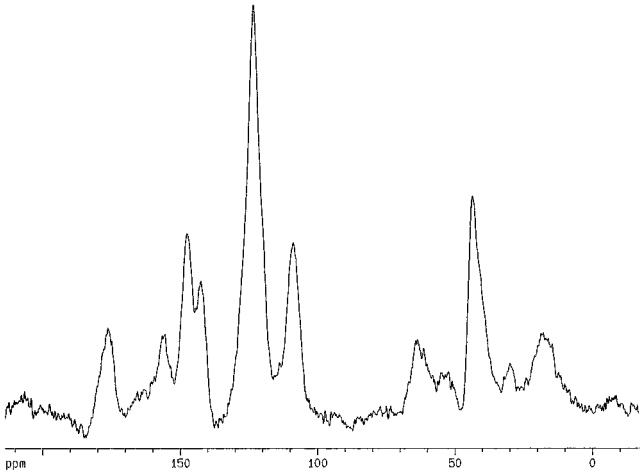

Figure 2. ^{13}C-CPMAS-NMR spectrum of pCARBA in conditions described in the Experimental Section. The chemical shifts are referenced to external adamantane.

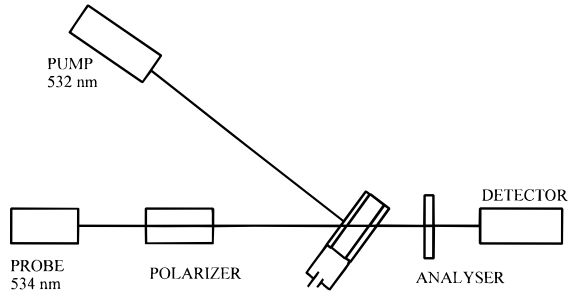

Figure 3. Experimental setup to determine electrooptic activity.

and 8 of the carbazole) and carbons 4a and 5a; 110 ppm, carbons 1 and 8 of the carbazole ring; 65−50 ppm, the NCH_2-CH_2O group; 47 ppm, the nonprotonated and methylene main-chain carbons; and 20 ppm, the α-methyl carbons.

The thin films of the polymer were obtained by dissolving the polymer in THF and spin-coating onto clean glass slides or onto indium tin oxide (ITO) coated glass substrates. The films were allowed to dry and subsequently heated to about 100 °C to drive off residual solvent. Relatively homogeneous thin films from 200 to 600 nm thickness were obtained by this procedure. A semitransparent layer of gold was vapor-deposited on the surface of the polymer film when required.

Electrooptical Effect and Photoconductivity. Photorefractivity may be present in photoconductive materials with electrooptic activity.[24] The electrooptic response was investigated on a pCARBA sandwich, prepared by casting a pCARBA solution in THF onto an ITO substrate, drying at 80 °C for about 10 h, and then depositing gold onto the film. The setup used is shown in Figure 3 and makes use of photoinduced poling at room temperature. The circularly polarized pump beam is used to orient a majority of the azocarbazole groups in the plane of the film, and the resulting signal through the cross-polarizers is set at zero, meaning that no chromophores are aligned along the electric field (which is not turned on in the initial step). Then, while maintaining the circularly polarized light on, the electric field (100 V/μm) is turned on and produces a signal on the detector. When the electric field is turned off, the signal on the detector returns to zero. The appearance of the signal demonstrates that optical poling has taken place under the electric field, and that translates into electrooptic activity for pCARBA.[25] Since the azocarbazole chromophore is structurally similar to previously reported azo chromophores, all showing electrooptic activity, this result is not unexpected.

Photoconductivity was measured in similarly prepared sandwich samples of pCARBA in the green (532 nm) and in the red (633 nm). The cell was biased with a dc voltage of up to 30 V and was illuminated through the ITO electrode. The photoconductivity was determined by measuring the photocurrent through the film. A linear dependence of log (normalized photocurrent) on the applied field was established. The normalized photocurrent is about 1 order of magnitude higher for illumination at 532 nm in comparison to 633 nm. Since most carbazole-containing polymers are photoconductive, it is not surprising that pCARBA is photoconductive as well.

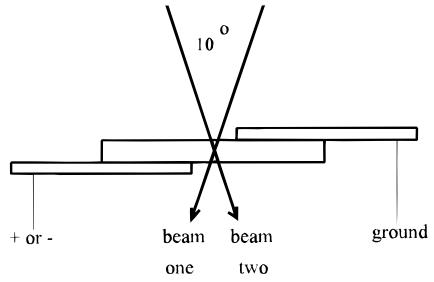

Figure 4. Experimental setup and irradiation geometry for photoinduced poling and photorefractive gratings inscription.

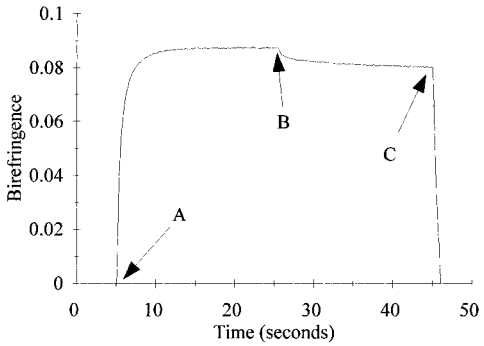

Figure 5. Optically induced and erased birefringence of pCARBA with a laser beam at 488 nm: (A) linearly polarized beam on; (B) beam off; (C) circularly polarized beam on.

Asymmetrical Two-Beam Gain Coupling. The sample cells for 2BC were prepared with the external field applied in either the film plane or normal to it. In the first case, the polymer was spin cast onto a glass slide partially vapor-deposited with silver. A second layer of silver was subsequently deposited on the top of the polymer film, leaving a gap large enough for two beams to intersect. In the second case, ITO slides were spin coated with pCARBA and then a semitransparent layer of gold was vapor-deposited on the entire surface. The cells were affixed to a transparent sample holder and electrodes attached to both the ITO and the gold layer, such that a +/− 0 to 80 V/μm electric field could be held across the polymer normal to the film surface. Two attenuated, equal-intensity, linearly polarized 543 nm beams from a He−Ne laser were crossed on the sample as per Figure 4, or the experimental set-up and sample geometry described by Yu.[26] In the case of the ITO samples, the beams were incident on the Au surface to eliminate interfering reflections throughout the sample volume and passed through the ITO layer and into a photodiode. The intensity of each beam could then be monitored over time as the other beam was introduced, removed, and reintroduced.

Results and Discussion

Optically Induced Birefringence. The GPC indicated an equivalent molecular weight of 9400. From the DSC, the polymer glass transition temperature (T_g) was found to be 160 °C and the start of decomposition was at 260 °C. The polymer film has maximum absorbance at 428 nm, which is much lower than the pseudostilbene type azo polymers we have studied so far. This indicates that the carbazolyl is a weaker electron donor compared with the aminophenyl group. The occurrence of λ_{max} at lower wavelength also suggests that the dipole moment of the azocarbazole group is smaller.

Figure 5 presents the writing−erasing curve for pCARBA. At point A, the linearly polarized writing

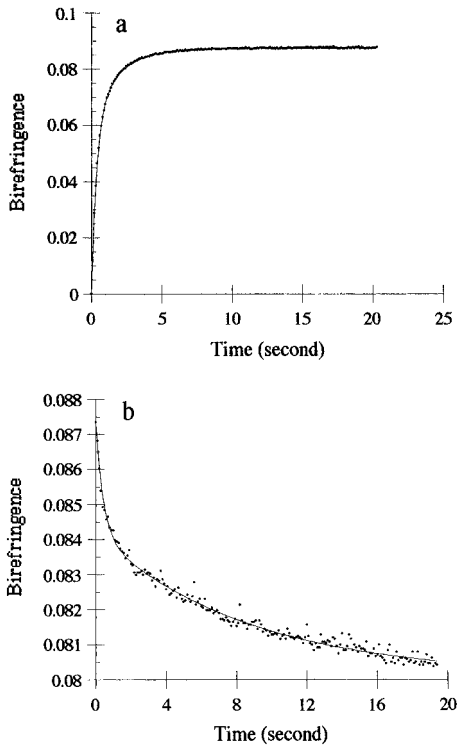

Figure 6. (A) Optically induced birefringence curve (points). The solid line is a fit to a biexponential function (eq 1) (B) Decay of birefringence after the laser is turned off (points). The solid line is a fit to a biexponential function (eq 2).

laser beam is engaged and the photoinduced birefringence is rapidly built up to the saturation level. At point B, the writing laser beam is removed and the birefringence begins to drop to a relaxed level where the rate of change of anisotropy is very small. At point C, a circularly polarized laser beam is turned on to randomize the orientation of the azo groups; hence, the anisotropy induced by the linearly polarized writing beam is destroyed.

The mechanism of inducing birefringence is based on the selective photochemical excitation of trans azocarbazole groups having a component of their dipole in the same direction as the laser polarization. Every trans azocarbazole group goes through many trans−cis−trans photoisomerization cycles, accompanied by changes in orientation, and—due to the selectivity of excitation—the orientation perpendicular to the laser polarization (which is not photochemically activated) will increase its population, creating dichroism and thus birefringence. Circularly polarized light activates all azocarbazole groups, thus restoring the initial random orientation. This mechanism is well known in the literature.[2]

As shown in Figure 5, the saturation value of the optically induced birefringence is 0.09, which is slightly lower than that of pDR1M.[19] Although the bulky azocarbazole moiety could in principle increase the conformational rigidity of the macromolecules and magnify the dichroic effect, a lower optically induced birefringence is observed. In fact, it has been observed that the replacement of phenyl by a naphthyl ring in the azo polymers does not show a significant effect on the induced dichorism,[19] and chiroptical properties.[27] The lower optically induced birefringence of pCARBA may be due to the smaller dipole moment of the azocarbazole group. More detailed studies of the effect of the dipole moment on the optical properties will be discussed in forthcoming publications.

The most distinguishable feature of the writing−erasing curve for pCARBA is the stability of the optically induced birefringence. Compared with other azo polymers studied earlier in our laboratory, in which the optically induced birefringence decreased to 60−80% of the saturation value after the writing laser was turned off, pCARBA only showed a 10% decrease after relaxation. The glass transition temperature of the polymer is very important for the storage stability, because the stability of the birefringence is obviously related to the ability of the azobenzene groups to reorient and randomize their distribution by slow motion in time. The higher the T_g of the polymer, the more unlikely this motion will be. The stability of the birefringence is consistent with the high glass transition temperature of pCARBA. In fact, the T_g of pCARBA is higher than those of the azo polymers reported earlier in our laboratory.

Table 1. Parameters Obtained by Fitting the Birefringence Growth Curves and Decay Curves to eq 1 and eq 2 Respectively

	wavelength of laser beam	
	514 nm	488 nm
k_a	1.51 ± 0.02	2.66 ± 0.04
k_b	0.33 ± 0.01	0.54 ± 0.01
A	0.056 ± 0.001	0.061 ± 0.001
B	0.030 ± 0.001	0.026 ± 0.001
A_n	0.65	0.70
B_n	0.35	0.30
k_c	0.59 ± 0.04	2.36 ± 0.19
k_d	0.029 ± 0.004	0.11 ± 0.01
C	0.0043 ± 0.0001	0.0032 ± 0.0001
D	0.0051 ± 0.0003	0.0041 ± 0.0001
E	0.078 ± 0.001	0.080 ± 0.001
C_n	0.05	0.04
D_n	0.06	0.05
E_n	0.89	0.91

[a] $A_n = A/(A + B)$; $B_n = B/(A + B)$; $C_n = C/(C + D + E)$; $D_n = D/(C + D + E)$; $E_n = E/(C + D + E)$.

Laser beams with wavelength 514 nm (0.7 W/cm^2) and 488 nm (1.1 W/cm^2) were used to photoinduce orientation on the same polymer film. Although the saturation value and the stable value are the same in both cases, the birefringence growth rate and the relaxation rate are significantly different. For a semiquantitative description of the photoinduced orientation and relaxation behavior at different writing laser wavelengths, the growth and relaxation of the birefringence were characterized by the following biexponential equations:

$$y = A(1 - \exp(-k_a t)) + B(1 - \exp(-k_b t)) \quad (1)$$

$$y = C \exp(-k_c t) + D \exp(-k_d t) + E \quad (2)$$

As reported previously, the biexponential functions gave a good fit to the growth and relaxation curves (Figure 6). The fitting parameters obtained are summarized in Table 1. As shown in Table 1, the polymer film showed a faster growth in birefringence for the 488 nm writing beam. This observation is reasonable because the polymer has a larger absorption coefficient at 488 nm and the intensity of the writing beam is higher at 488 nm (Figure 7). The larger absorption coefficient and higher writing intensity give rise to a faster trans−cis−trans isomerization rate and hence faster achievement of the saturation value. In addition to the faster trans−cis−trans isomerization rate, the 488 nm writing beam might also increase the temperature of the sample more than the 514 nm beam, thus resulting in an increased mobility of the chromophores and the polymer chains. Besides the faster writing rate, a faster decay was also observed when the sample was written by the 488 nm laser beam. The faster decay is

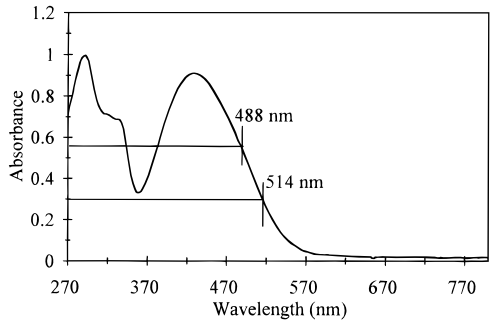

Figure 7. UV-vis spectrum of the pCARBA film.

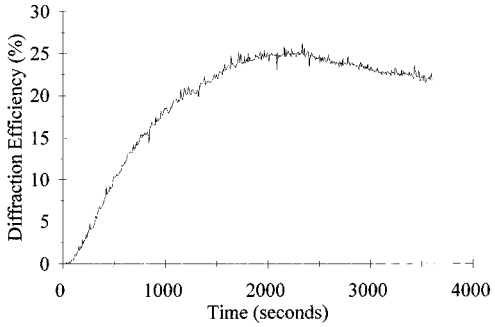

Figure 8. Diffraction efficiency of surface gratings inscribed on the pCARBA film as a function of time. The writing beam is at 514 nm and the intensity is 19 mW/cm^2.

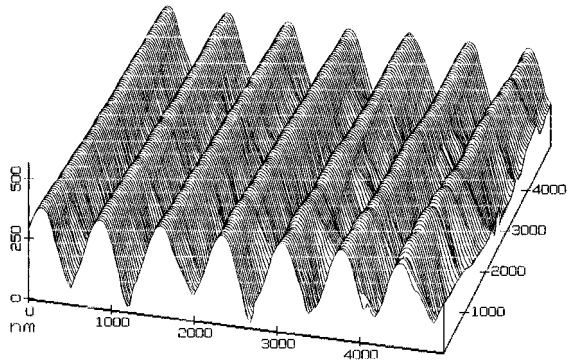

Figure 9. Atomic force microscope surface profile of the pCARBA film.

probably due to the thermal effect of the laser beam or to the greater amount of cis remaining when the beam is turned off.

The remnant birefringence (E_n) is higher than what was obtained in previous systems,[19] confirming that the stability of the photoinduced orientation is greater in a more aromatic system, due to the presence of the carbazole ring.

Optically Induced Diffraction Grating. Figure 8 shows the time dependence of the diffraction efficiency for an optically induced grating experiment carried out at an intensity of 19 mW/cm^2. As shown in Figure 8, the diffraction efficiency goes up to about 25% after 2000 s and starts to decrease after 2400 s. The decrease of diffraction efficiency after prolonged exposure to the laser beam is common to most of our azo polymers and is probably due to some decomposition of the pCARBA.

The grating produced is permanent as long as the sample's temperature is kept below T_g. The surface profile of the film after the creation of the grating was studied by atomic force microscopy. The result is presented in Figure 9. The grating profile exhibits a sinusoidal shape, with a grating depth of about 300 nm and grating spacing of about 700 nm.

Surface grating formation by the interference of two laser beams has only recently been reported in the literature.[7, 8] Whole polymer chains must be moved through the volume of the film in order to produce gratings over 100 nm deep, and the mechanism of such significant mass transport below T_g is believed to be based on the pressure induced by photoisomerization.[28] The temperature plays an important role in this phenomenon but is not the most important factor.

Apart from the obvious uses of the photoinduced birefringence and surface gratings inscription in optical storage devices, especially holographic storage, applications such as erasable waveguides and optical couplers into films (using the excellent diffraction efficiency) of the grating can also be envisaged.[29]

Asymmetric Two-Beam Gain Coupling. Irradiation of the sample as described has been shown to produce a transient absorption grating, stable yet reversible birefringence grating, and—under proper conditions—an irreversible surface profile grating. All of these gratings will diffract a probe beam (including the pump beams) to first or higher orders, yet are field independent. In addition, beam gain from one or a combination of these gratings due to multiwave mixing will necessarily be symmetric if the incident beams are of equal intensity, with each of the two pump beams experiencing loss and gain to the same degree when coincident. Net gain through this mechanism can only be achieved if the two input beams have significantly different intensities. Experiments to investigate this phenomenon are underway.

The photorefractive gratings investigated here are a result of a nonlinear optical (NLO) effect when an electric field is applied to the poled polymer with a component parallel to the grating wavevector. The polymer film was poled at room temperature by irradiation with a circularly polarized beam close to the absorbance maximum, from 488 to 543 nm. The light was circularly polarized, to provide a uniform intensity of about 50 mW/cm^2 for isomerization and hence for the motion required for the material to respond to the applied field and align below T_g. To form the photorefractive grating, the two 0.5 mW 543 nm beams were linearly p-polarized and the field left on. The field could then be reversed and the material repoled, and a new photorefractive grating inscribed and monitored. In this way, the gratings could be written and the intensity of each beam monitored for net loss or gain with selective introduction of the other and as a function of the field direction. Asymmetric 2BC, which reverses with reversed field direction, is a phenomenon limited to photorefractive systems and serves as proof of the effect as well.[24] As the asymmetric 2BC measurements are carried out on thin films at an absorbing wavelength, estimates of the beam coupling energy transfer coefficient could not be made accurately. Further work for a quantitative estimate of the 2BC will have to be carried out on polymers similar to pCARBA containing longer spacers, better suited for thick-film preparation, at wavelengths which are less absorbing. We could not prepare a thick film of pCARBA of good optical quality for such measurements.

Asymmetric 2BC as proof of photorefractivity is illustrated in Figure 10, a composite of four separate experiments. This was achieved with the samples holding the applied field parallel to the film surface, as shown in Figure 4, as they held charge more reliably without degradation for reproducibility. The asymmetric 2BC was also demonstrated on the ITO samples with the field applied normal to the surface. The

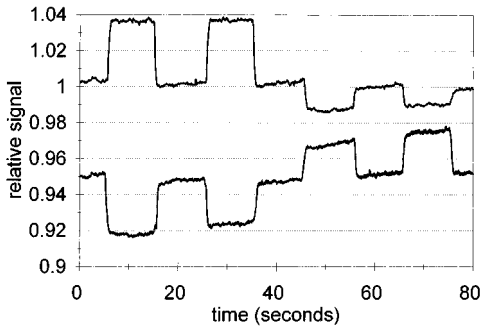

Figure 10. Asymmetrical 2BC of beam 1 (upper trace) and beam 2 (lower trace) with a +5 V/μm field (first half) and −5 V/μm field (second half).

reflected beam (beam 1) is monitored with the nonreflected beam (beam 2) removed as a +5 V/μm electric field is applied. Beam 2 is introduced twice for 10 s at $t = 5$ and $t = 25$ s (upper curve), illustrating a gain in relative signal of 4%. Beam 2 is then monitored in the same field while beam 1 is similarly twice introduced and removed, showing a corresponding loss of 4% of the relative signal (lower curve). The two beams are of equal intensity but offset 0.05 for clarity. The field is then reversed to −5 V/μm and beam 1 (upper curve, second half) now shows a loss with the coincidence of beam 2, and beam 2 now exhibits gain (second half of lower curve). Alignment of the electrooptic side chain chromophores is achieved using the photochemical trans−cis−trans isomerization and orientation of the azo groups in the presence of the electric field instead of high-temperature poling.

This material has the advantages of completely polymeric photorefractives, such as high component loading concentrations, high T_g, and stability against phase separation. Fully polymeric photorefractive systems have been prepared, measured and previously reported,[30, 31] mainly with a backbone functionalized with separate NLO chromophores, charge generators, and charge transporters. While these systems allow tailoring of relative component concentrations, problems are often encountered with charge transport groups being too distant from each other and general dilution of each component by the others.[24] The photorefractive effect has been previously reported on a copolymer where there was a single active component of the (dialkylamino)nitrostilbene type.[32] In that case, the amino substituent on the stilbene was believed to be responsible for the photoconductivity of the polymer. However, the photorefractive nature of the results was questioned, because asymmetric 2BC experiments were not reported.[26]

Conclusions

An azo polymer with side chain azocarbazole was synthesized, and the optically induced birefringence and diffraction gratings were studied. The optically induced birefringence obtained is slightly lower than that of the pseudostilbene type azo polymers studied previously; however, it is comparatively more stable. Asymmetrical two-beam gain coupling was demonstrated as proof of the photorefractive effect.

Probably the most important property of the pCARBA film is that it is amenable to all three processes described. It is thus possible to imagine a polymer film on which waveguides could be written and erased with a laser, which has points of entry and exit of light into these waveguides by optically induced surface gratings on the film and has the switching capability given by the photorefractive property. At least in theory, a single polymer film could be used as a multifunctional photonic device. This possibility is being explored in our laboratory.

Acknowledgment. Funding from the Office of Naval Research, NSERC Canada, and the Department of Defense Canada is gratefully acknowledged. A.N. thanks Canada Council for a Killam Research Fellowship.

References and Notes

(1) Xie, S.; Natansohn, A.; Rochon, P. *Chem. Mater.* **1995**, *5*, 403.
(2) Natansohn, A.; Rochon, P.; Gosselin, J.; Xie, S. *Macromolecules* **1992**, *25*, 2268.
(3) Natansohn, A.; Rochon, P.; Xie, S. *Macromolecules* **1992**, *25*, 5531.
(4) Rochon, P.; Gosselin, J.; Natansohn, A.; Xie, S. *Appl. Phys. Lett.* **1992**, *60*, 4.
(5) Rochon, P.; Bissonette, D.; Natansohn, A.; Xie, S. *Appl. Opt.* **1993**, *32*, 7277.
(6) Natansohn, A.; Rochon, P.; Pezolet, M.; Audet, P.; Brown, D.; To, S. *Macromolecules* **1994**, *27*, 2580.
(7) Rochon, P.; Batalla, E.; Natansohn, A. *Appl. Phys. Lett.* **1995**, *66*, 136.
(8) Kim, D. Y.; Tripathy, S. K.; Li, L.; Kumar, J. *Appl. Phys. Lett.* **1995**, *66*, 1166.
(9) Sekkat, Z.; Dumont, M. *Appl. Phys. B* **1992**, *54*, 486.
(10) Blanchard, P. M.; Mitchell, G. R. *Appl. Phys. Lett.* **1993**, *63*, 2038.
(11) Bauer-Gongonea, S.; Bauer, S.; Wirges, W.; Gerhard-Multhaupt, R. *J. Appl. Phys.* **1994**, *76*, 2627.
(12) Ducharme, S.; Scott, J. C.; Twieg, R. J.; Moerner, W. E. *Phys. Rev. Lett.* **1991**, *66*, 1846.
(13) Prasad, P. N.; Orczyk, M. E.; Zieba, J. *J. Phys. Chem.* **1994**, *98*, 8699.
(14) Hadziioannou, G.; Bolink, H. J.; Krasnkov, V. V. *Adv. Mater.* **1994**, *6*, 574.
(15) Silence, S. M.; Donckers, M. C. J. M.; Walsh, C. A.; Burland, D. M.; Twieg, R. J.; Moerner, W. E. *Appl. Optics* **1994**, *33*, 2218.
(16) Kippelen, B.; Tamura, K.; Peyghambarian, N.; Padias, A. B.; Hall, H. K., Jr. *J. Appl. Phys.* **1993**, *74*, 3617.
(17) Tamura, K.; Padias, A. B.; Hall, H. K., Jr.; Peyghambarian, N. *Appl. Phys. Lett.* **1992**, *60*, 1803.
(18) Meerholz, K.; Volodin, B.; Sandalphon; Kippelen, B.; Peyghambarian, N. *Nature* **1994**, *371*, 497.
(19) Ho, M. S.; Natansohn, A.; Rochon, P. *Macromolecules* **1995**, *28*, 6124.
(20) Moylan, C.; Twieg, R.; Lee, V.; Swanson, S.; Betterton, K.; Miller, R. *J. Am. Chem. Soc.* **1993**, *115*, 12599.
(21) Verbiest, T.; Burland, D. M.; Jurich, M. C.; Lee, V. Y.; Miller, R. D.; Volksen, W. *Macromolecules* **1995**, *28*, 3005.
(22) Ellwood, M.; Griffiths, J. *J. Chem. Soc., Chem. Commun.* **1980**, 181.
(23) Kobayashi, H.; Sonoda, T.; Iwamoto, H.; Yoshimura, M. *Chem. Lett.* **1981**, 579.
(24) Moerner, W. E.; Silence, S. M. *Chem. Rev.* **1994**, *94*, 127.
(25) Schildkraut, J. S. *Appl. Opt.* **1990**, *29*, 2839.
(26) Yu, L.; Chan, W. K.; Peng, Z.; Gharavi, A. *Acc. Chem. Res.* **1996**, *29*, 13.
(27) Angiolini, L.; Caretti, D.; Carlini, C. *J. Polym. Sci., Part A: Polym. Chem.* **1994**, *32*, 1159.
(28) Barrett, C. J.; Natansohn, A. L.; Rochon, P. L. *J. Phys. Chem.*, in press.
(29) Ho, M. S.; Barrett, C.; Rochon, P.; Natansohn, A. *Organic Thin Films for Photonic Applications; OSA Tech. Digest Ser.* **1995**, *21*, 338.
(30) Yu, L.; Chan, W.; Bao, Z.; Cao, S. X. F. *Macromolecules* **1993**, *26*, 2216.
(31) Peng, Z.; Bao, Z.; Yu, L. *J. Am. Chem. Soc.* **1994**, *116*, 6003.
(32) Sansone, M. J.; Teng, C. C.; East, A. J.; Kwiatek, M. S. *Opt. Lett.* **1993**, *18*, 1400.

MA951432A